Cooperative Motion Planning for Multiple Autonomous Marine Vehicles ⋆

Andreas J. Häusler * **Alessandro Saccon** * **A. Pedro Aguiar** *
John Hauser ** **António M. Pascoal** *

* *Instituto Superio Técnico, Lisboa, Portugal*
{ahaeusler,asaccon,pedro,antonio}@isr.ist.utl.pt
** *University of Colorado at Boulder, Boulder, USA*
john.hauser@colorado.edu

Abstract: There is widespread interest in the deployment of fleets of marine robots with the potential to roam the oceans freely and collect data at an unprecedented scale. This calls for the development of efficient algorithms for multiple vehicle motion planning that can take directly into account the capabilities of each vehicle and environmental conditions and lend themselves to seamless integration with control and navigation systems. The paper describes advances towards the development of a new breed of motion planning systems that address explicitly inter-vehicle collision avoidance, together with a number of criteria that may include simultaneous times of arrival at assigned target points, energy minimization, and acoustic communication constraints. The theoretical framework adopted is rooted in the so-called Projection Operator Approach that borrows from optimization and dynamical systems theory. Simulations with full dynamic vehicle models illustrate the potential of the methods developed.

Keywords: Trajectory Optimization, Trajectory Generation, Multiple Autonomous Marine Vehicles, Projection Operator, Energy-Minimal Optimization, Collision Avoidance, Obstacle Avoidance.

1. INTRODUCTION

Marine robotics is a highly active and rapidly evolving field of research, and recent advances have made it both technologically and economically possible to execute missions involving more than one vehicle. This opens up new avenues for marine research that were not possible before, for it increases drastically the interest in applications where multiple autonomous marine vehicles (AMVs) execute missions at sea cooperatively, in order to achieve new and challenging goals.

1.1 Cooperative Planning for Multiple AMVs

It is nowadays at the heart of most research programs to fully explore the possibilities that multiple AMV scenarios pose, and, in accordance with that, the areas of application are widespread and diverse. One of the most explored scenarios to date is the sampling of ocean data (Leonard et al., 2010; Ögren et al., 2004), and it is a subject of continuous interest how to optimize a cooperative mission in terms of maximizing the amount of collected samples.

Another active field of research is the incorporation of heterogeneous AMVs into one cooperative framework for mission execution (Aguiar et al., 2009). Several factors need to be taken into account, and besides having to solve the obvious problem of finding a common framework upon which inter-vehicle communication can be based, a mission has to be planned in such a manner that the constraints imposed by the vehicles' different dynamics are taken into account to yield feasible trajectories and therefore, an executable mission.

Recent advances in diver assistance and harbor security scenarios (Indiveri et al., 2010) also demonstrate the importance of cooperation among the vehicles. Providing the diver unit with means of trilateration, i.e. positional information and directional instructions in relation to the mission objectives, not only requires a reliable control that is capable of adapting the vehicle formation in case the diver diverges from its path. It also inherently requires a mission plan that brings together the mission objectives and the vehicle restrictions and outputs a mission that is optimal in vehicle energy usage as well as in terms of the strain put on the diver when following the instructions transmitted to him by the assisting vehicle network.

1.2 Related Work

In Paley et al. (2008), trajectories are designed to meet the scientific objectives of a mission, and adapted in case of vehicle failures. Instead of aiming for single-track trajectories with simultaneous arrival, the objective is rather a closed shape that can be executed repeatedly; if more than one vehicle follows such a trajectory, they need to maintain a fixed distance. Vehicle models are explicitly incorporated, but used only for position prediction; trajectory planning is done using a simplified point-mass model.

Spangelo and Egeland (1994) use optimal control techniques for path planning with respect to minimum energy requirement, where the energy is computed as the mechanical power input

⋆ Research supported in part by projects MORPH of the EU FP7 (grant agreement no. 288704) and CONAV of the FCT (contract number PTCD/EEA-CRO/113820/2009), and by the FCT Program PEst-OE/EEI/LA0009/2011.
The work of A. Häusler was supported by a Ph.D. scholarship of the FCT under grant number SFRH/BD/68941/2010.
This work was completed while A. Häusler was a visiting scholar at the University of Colorado at Boulder, USA.

to the propeller shaft, which, according to Kumar et al. (2005), means that the performance index does not exactly represent the energy consumed by the thrusters. By defining path constraints, the trajectories are planned in a way that obstacles are avoided. The vessel model is explicitly incorporated. This is also done by Inanc et al. (2005), but here, energy-minimal trajectories are computed by assuming the instantaneous power to be constant.

1.3 Contribution

In previous publications (see Häusler et al. (2010) and the references therein), we restricted ourselves to a kinematic model of the vehicles under consideration. Optimization constraints related to the dynamics had to be incorporated indirectly by constraining the kinematic model, e.g. by providing numerical bounds on the path's curvature.

In this paper, we introduce a novel approach to cooperative planning and optimization of energy-minimal trajectories in the presence of obstacles. The trajectories are guaranteed to be feasible in terms of the vessels' dynamic models, which is an advantage inherent to the projection-operator based optimization approach we follow, since it explicitly incorporates the vessel dynamics. A minimum energy planning problem is solved to obtain the trajectories, with an emphasis on the computation of the energy as the integral of the instantaneous power drained from the batteries , i.e. electrical (and not the more commonly used mechanical) power.

The paper is organized as follows: we first summarize the dynamic model for the MEDUSA class of autonomous surface vehicles in Sec. 2, where we also introduce the accompanying static equations that, as part of the cost function, achieve energy expenditure minimization. We discuss the problem formulation in relation to that vehicle model in Sec. 3, before giving an overview of the optimization approach in Sec. 4. The paper concludes with simulation results in Sec. 5, after which final comments and the research outlook are included in Sec. 6.

2. THE MEDUSA MODEL

The MEDUSA ASV is a vessel recently developed at the Dynamical Systems and Ocean Robotics laboratory at ISR/IST in Lisbon. Its hull consists of two torpedo shaped tubes that lie parallel to the water surface, but with a vertical displacement, so that one tube is fully submerged at all times. By switching off the GPS receiver, this design even allows treating the MEDUSA as if it were an underwater vehicle (in some limited fashion), while still making it possible for the operator to observe an ongoing mission directly, thus making the MEDUSA an ideal test platform for the development of planning algorithms, cooperative controllers, and more.

2.1 Kinematic and Dynamic Equations

Since the MEDUSA is conceptually a semi-submersible, the mathematical model can be considered to be that of a planar vehicle. Using the notation of Fossen (2002), the model is

$$\dot{\eta} = R(\eta)\nu \tag{1}$$

$$\big(M_{\text{rb}} + M_{\text{a}}\big)\dot{\nu} + \big(C_{\text{rb}}(\nu) + C_{\text{a}}(\nu)\big)\nu + \big(D + D_{\text{n}}(\nu)\big)\nu = \tau \tag{2}$$

where the kinematic states $\eta = [x, y, \psi]$ express the vessel's pose in the inertial reference frame $\{I\}$, and the dynamic state

Fig. 1. The MEDUSA vessel set-up. The thrusters are mounted in the middle between both hull parts on the x-z-plane (body coordinates) and produde completely from the body on the x-y-plane.

vector $\nu = [u, v, r]$ represents the velocities in the body frame $\{B\}$. In (1), $R(\eta)$ is a rotation matrix such that

$$\begin{bmatrix}\dot{x}\\ \dot{y}\\ \dot{\psi}\end{bmatrix} = \begin{bmatrix}\cos\psi & -\sin\psi & 0\\ \sin\psi & \cos\psi & 0\\ 0 & 0 & 1\end{bmatrix}\begin{bmatrix}u\\ v\\ r\end{bmatrix}$$

The model inputs n_{ps} and n_{sb} are the rotational velocities of the MEDUSA's actuators, the port side and starboard propeller, respectively, obtained by multiplying a percentage command with the maximally admissible rotational velocity n_{max}. Maneuvering is done using common and differential thrust, resulting in the external force vector

$$\tau = \begin{bmatrix} T_{\text{ps}} + T_{\text{sb}} \\ 0 \\ l(T_{\text{ps}} - T_{\text{sb}}) \end{bmatrix}$$

where l is the displacement of the propellers from the center of $\{B\}$, see Fig. 2. The forces T_{ps} and T_{sb} are functions of u, r, and the two propellers' rotational velocities, n_{ps} and n_{sb}, respectively, both given in [rps].

Placing the center of $\{B\}$ at the center of mass of the vessel, the rigid body and hydrodynamic added mass matrices in the dynamics (2) can be written as

$$M_{\text{rb}} = \begin{bmatrix} m & 0 & 0 \\ 0 & m & 0 \\ 0 & 0 & I_{zz} \end{bmatrix} \quad M_{\text{a}} = -\begin{bmatrix} X_{\dot{u}} & 0 & 0 \\ 0 & Y_{\dot{v}} & 0 \\ 0 & 0 & N_{\dot{r}} \end{bmatrix}$$

where m is the body mass and I_{zz} the rigid body inertia. The rigid body and hydrodynamic centripetal and Coriolis matrices are

$$C_{\text{rb}}(\nu) = \begin{bmatrix} 0 & -mr & 0 \\ mr & 0 & 0 \\ 0 & 0 & 0 \end{bmatrix} \quad C_{\text{a}}(\nu) = \begin{bmatrix} 0 & 0 & -Y_{\dot{v}}v \\ 0 & 0 & X_{\dot{u}}u \\ Y_{\dot{v}}v & -X_{\dot{u}}u & 0 \end{bmatrix}$$

and the linear and nonlinear drag is expressed as

$$D = -\begin{bmatrix} X_u & 0 & 0 \\ 0 & Y_v & 0 \\ 0 & 0 & N_r \end{bmatrix} \; D_{\text{n}}(\nu) = -\begin{bmatrix} X_{|u|u}|u| & 0 & 0 \\ 0 & Y_{|v|v}|v| & 0 \\ 0 & 0 & N_{|r|r}|r| \end{bmatrix}$$

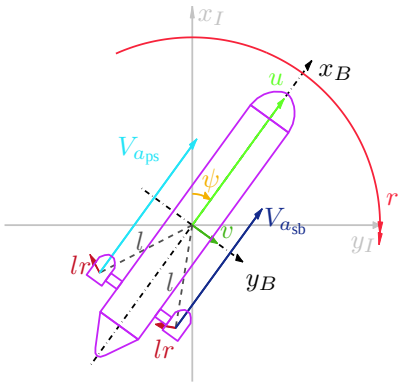

Fig. 2. Conceptual drawing of the MEDUSA as seen from above. The arrows illustrate the velocities experienced at different points of the body for a system that is undergoing a right turn with $r = 0.1\text{s}^{-1}$ while moving forward with $u = 1.0\text{ms}^{-1}$. The black coordinate axes represent the body frame $\{B\}$, the grey axes the inertial frame $\{I\}$.

2.2 Static Equations for Thrust and Torque

Since the model inputs are the propellers' rotational velocities n_{ps} and n_{sb}, a mapping between those and the thrust T_{ps} and T_{sb} needs to be defined. The standard way is given through the *open-water coefficients* (Fossen, 2002). It turns out, however, that models based on these coefficients are only applicable in the regime of non-zero advance velocity at the propeller blade, together with non-zero propeller velocities, where the rotational direction must be the one that drives the vessel forward. This is because the coefficients are defined in terms of the open-water advance ratio $J_{\text{o}} = \frac{v_{\text{a}}}{nd}$, where v_{a} is the propeller's (and the vessel's) advance speed, n is the rotational velocity of the propeller, and d is its diameter. Clearly, a zero-crossing of the propeller speed makes the advance ratio go to infinity.

Thus, for small ocean vehicles, especially ones that are steered by differential thrust from two or more propellers (and not, for instance, by changing the deflection of a rudder), another model must be used, as it is highly likely that the propellers will change their rotational direction for maneuvers that involve curved trajectories. A model that is valid for all regions of motion (i.e. ahead, back, crash back and crash ahead) is described by van Lammeren et al. (1969) and explored later on by Oosterveld (1970) and Bachmayer et al. (2000), the so-called *four-quadrant model*. The coefficients used by this model are given in terms of the advance angle β at the propeller blade, and data is available in the form of a 20th order Fourier series for various ducted propellers and nozzles (Oosterveld, 1970). A smoothing procedure that makes the coefficients more usable for Newton descent methods is described in Healey et al. (1994).

In this propeller model, the thrust and torque equations are

$$T = \frac{1}{2}\rho c_{\text{T}}(\beta)\left(v_{\text{a}}^2 + v_{\text{p}}^2\right)\pi R^2 \tag{3}$$

$$Q = \frac{1}{2}\rho c_{\text{Q}}(\beta)\left(v_{\text{a}}^2 + v_{\text{p}}^2\right)\pi R^2 d \tag{4}$$

where d is the propeller diameter and $R = d/2$ is its radius. The advance angle can be computed as

$$\beta = \text{atan2}(v_{\text{a}}, v_{\text{p}}) \tag{5}$$

where v_{a} is the advance velocity of the propeller, and v_{p} is the lateral velocity of the propeller blade at radius $0.7R$, which is a function of the rotational velocities. See Fig. 3, and Bachmayer et al. (2000) and Healey et al. (1994) for an illustration of the concepts involved. In what follows,

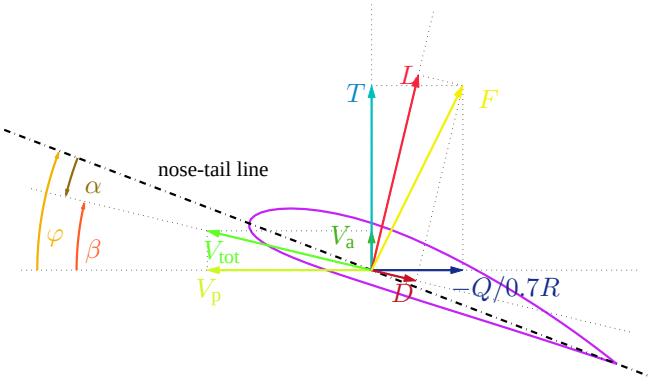

Fig. 3. A cross-section of the propeller blade at $0.7R$ showing the forces and velocities acting on the propeller blade (the force vectors are enlarged). The propeller runs counter-clockwise in order to achieve forward thrust T, moving the system upwards in this picture. To avoid overlapping arrows, the tangential component of the propeller torque Q at $0.7R$ is shown here with a negative sign. Propeller lift L and drag D and total hydrodynamic force F are only shown for reference.

$$v_{\text{p}_{\text{ps,sb}}} = 0.7R\omega_{\text{ps,sb}} = 0.7R2\pi n_{\text{ps,sb}} \tag{6}$$

When the vessel is rotating about the z axis, we need to account for the fact that the advance velocities at the propellers are different from each other, which results in the side-dependent expressions

$$\begin{aligned} V_{\text{a}_{\text{ps}}} &= \sin(\text{atan2}(-p_y, p_x))lr + u = -p_y r + u \\ V_{\text{a}_{\text{sb}}} &= \sin(\text{atan2}(p_y, p_x))lr + u = p_y r + u \end{aligned} \tag{7}$$

Here, (p_x, p_y) is the offset of the propellers from the vessel's center of mass in body coordinates, and l is their absolute distance to the center of mass (see Fig. 2). Since (6) and (7) are dependent on the vessel side, it needs to be kept in mind that the advance angle (5) and both the thrust (3) and the torque (4) need to be computed separately for each propeller.

The MEDUSA vessel uses Seabotix HPDC1507 thrusters, which run in a Type 37 Kort nozzle and have a pitch ratio of roughly $P/d \approx 1.2$. A correction factor (the detailed derivation of which is not given here due to space limitations) was applied to achieve the bollard-pull conditions that Seabotix indicates for this thruster model. Thanks to the particular body shape of the MEDUSA (see Fig. 1), we may regard propeller-hull interactions as negligible and treat the propellers as if they were running in open water, simply employing the four quadrant model just described.

3. PROBLEM FORMULATION

Our goal is to generate trajectories for missions involving multiple MEDUSAs. The trajectories are required to be free of inter-vehicle collisions as well as collisions with obstacles. Furthermore, they must be optimal in terms of prospective energy usage throughout the mission, take into account the dynamic constraints of the vessel, and provide the means of simultaneous arrival.

When referring to minimum energy trajectories, the energy to be minimized is usually understood as the amount of work done to change the vehicle's velocity and overcome the drag forces (Kruger et al., 2007). Here, however, we are more in the line with Chyba et al. (2008), since we want the algorithm to find trajectories that are minimal in terms of the wattage drawn from the the batteries. To this effect, we formulate an additional set of static equations that are based on the DC motor model for the thrusters, and which will be used as means of computing the required electrical energy along a trajectory to allow for the

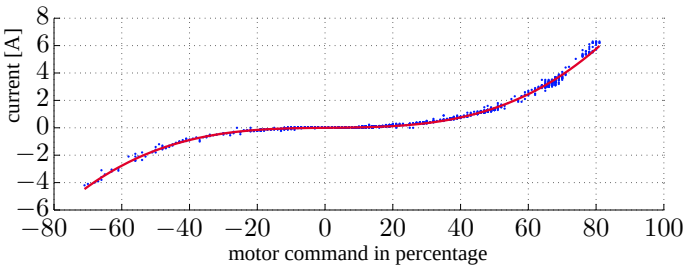

Fig. 4. Data and polynomial fit for the port-side motor, obtained from measurements conducted on April 14, 2011, data set of 09:46 am.

computation of energy-related quantities that make sense in a physically sound manner.

Since the terminal inductance of the thrusters is small ($L_a \approx 500\mu H$), we can neglegt the fast dynamics of the electric part of the standard DC motor equation, $L_a \frac{dI}{dt} + R_a I = V - K_e \omega$ (Franklin et al., 2002), and write the relation of the rotational velocities of the propellers to the voltage as

$$V_{\text{ps,sb}} = R_a I_{\text{ps,sb}} + K_e \omega_{\text{ps,sb}} = R_a I_{\text{ps,sb}} + K_e 2\pi n_{\text{ps,sb}} \quad (8)$$

where $V_{\text{ps,sb}}$, $I_{\text{ps,sb}}$ and R_a are the armature voltage, current and resistance of the (portside/starboard) DC motor, K_e is its electrical constant, and $n_{\text{ps,sb}}$ its rotational velocity. There is no data available on the viscous friction coefficient and the rotor inertia of the Seabotix thrusters, which would usually be required to compute the armature current I as a function of the rotational velocities from the mechanical part of the DC motor dynamics. However, we were able to determine the currents I_{ps} and I_{sb} as functions of n_{ps} and n_{sb}, respectively, from measurements conducted with the MEDUSA, and by fitting a 3rd order polynomial to the data obtained (see Fig. 4).

Considering the different inputs for port side and starboard propeller, the electrical power consumed by the motors thus is

$$\begin{aligned} P &= V_{\text{ps}} I_{\text{ps}} + V_{\text{sb}} I_{\text{sb}} + P_p \\ &= (R_a I_{\text{ps}} + K_e n_{\text{ps}}) I_{\text{ps}} + (R_a I_{\text{sb}} + K_e n_{\text{sb}}) I_{\text{sb}} + P_p \end{aligned} \quad (9)$$

with P_p as the constant power required by the on-board computers. This, under the assumptions made for (8), can of course only be applied if we have maneuvers that sustain the velocity for a certain amount of time; if the velocity changes faster, one has to be more sophisticated than using steady-state equations.

4. MATHEMATICAL FRAMEWORK

Before discussing the technical details of formulating the collision avoidance constraints, we give a very short overview of the projection operator method we adopt in this paper. The reader is referred to Hauser (2002) and related papers for in-depth detail.

4.1 The Projection Operator Approach and Barrier Functional

The central idea of this approach to the solution of optimal control problems is a *projection operator* method that allows expressing the dynamically constrained optimization problem

$$\begin{aligned} &\text{minimize} && \int_0^T l(x(\tau),u(\tau),\tau)\, d\tau + m(x(T)) \\ &\text{subject to} && \dot{x}(t) = f(x(t),u(t),t),\ x(0) = x_0 \end{aligned} \quad (10)$$

as an unconstrained one, and use Newton's method to find an optimal solution. This is centered around the realization that a trajectory tracking controller defines a function space *operator* that maps a desired trajectory (a *curve*) to a system *trajectory* (an element of the trajectory manifold). Composing the optimization objective (a *functional*) with the (trajectory tracking) *projection operator* converts the dynamically constrained optimal control problem into an essentially unconstrained optimization problem.

Suppose that $\xi(t) = (\alpha(t), \mu(t))$, $t \geq 0$, is a bounded curve (e.g., an approximate trajectory of f) and let $\eta(t) = (x(t), u(t))$, $t \geq 0$, be the trajectory of f determined by the nonlinear feedback system

$$\begin{aligned} \dot{x}(t) &= f(x(t),u(t),t), \qquad x(0) = x_0 \\ u(t) &= \mu(t) + K(t)(\alpha(t) - x(t)) \end{aligned}$$

This feedback system defines a continuous, nonlinear *projection operator*

$$\mathcal{P} : \xi = (\alpha(\cdot), \mu(\cdot)) \mapsto \eta = (x(\cdot), u(\cdot))$$

This allows us to formulate the following algorithm for infinite-dimensional optimization, similar to the Newton method for optimization of a function $g(\cdot)$, e.g., in finite dimensions:

PROJECTION OPERATOR NEWTON METHOD

1 **Init** initial trajectory $\xi_0 \in \mathcal{T}$
2 **for** $k = 0, 1, 2, \ldots$
3 **do** design feedback $K(\cdot)$ defining $\mathcal{P}$ about ξ_i
4 search direction
$\zeta_i = \arg\min_{\zeta \in T_{\xi_i}\mathcal{T}} Dh(\xi_i)\cdot\zeta + \frac{1}{2} D^2 g(\xi_i)\cdot(\zeta,\zeta)$
5 step size $\gamma_i = \arg\min_{\gamma \in (0,1]} g(\xi_i + \gamma\zeta_i)$
6 update $\xi_{i+1} = \mathcal{P}(\xi_i + \gamma_i \zeta_i)$

where $\mathcal{T}$ is the trajectory manifold, $\xi \in \mathcal{T}$, and $g(\xi) := h(\mathcal{P}(\xi))$ with

$$h(\xi) := \int_0^T l(\alpha(\tau),\mu(\tau),\tau)\, d\tau + m(\alpha(T))$$

Since our problem formulation demands having additional collision avoidance constraints, we have in fact a constrained optimal control problem

$$\begin{aligned} \min \quad & \int_0^T l(x(\tau),u(\tau),\tau) d\tau + m(x(T)) \\ \text{s.t.} \quad & \dot{x}(t) = f(x(t),u(t),t),\ x(0) = x_0 \\ & c_j(x(t),u(t),t) \geq 0, \quad t \in [0,T],\ j \in \{1,\ldots,k\} \end{aligned} \quad (11)$$

We incorporate the constraints $c_j(\cdot)$ using the barrier functional method introduced in Hauser and Saccon (2006). The method requires the approximate log barrier function $\tilde{\beta}_\delta(\cdot)$, $0 < \delta \leq 1$ defined as

$$\tilde{\beta}_\delta(z) = \begin{cases} -\log z & z > \delta \\ \dfrac{k-1}{k}\left[\left(\dfrac{z - k\delta}{(k-1)\delta}\right)^k - 1\right] - \log\delta & z \leq \delta \end{cases} \quad (12)$$

where $k > 1$ is an even integer. This allow us to express (11) in the shape of (10) as

$$\begin{aligned} \text{minimize} \quad & \int_0^T \Big(l(x(\tau),u(\tau),\tau) \\ & \qquad + \epsilon \sum_{j=1}^{k} \tilde{\beta}_\delta(c_j(x(\tau),u(\tau),\tau)) \Big)\, d\tau + m(x(T)) \\ \text{subject to} \quad & \dot{x}(t) = f(x(t),u(t),t),\ x(0) = x_0 \end{aligned}$$

where ϵ and δ express the "sharpness" of the barrier, and are reduced over the iterations of the algorithm to force the trajectories into the valid region of the optimization space.

We found it necessary to slightly modify (12), since it assumes (unbounded) negative values for $z > 1$. This may result in a domination of the negative part in the cost integral, thereby, in relation to our application, effectively putting a *reward* on staying away from the other vehicle (or obstacle) as far as possible in addition to the cost for avoiding collisions. Since this is not desirable, we extended (12) by forming a composition with the $\mathcal{C}^2$-smooth "hockey stick" function

$$\sigma(z) = \begin{cases} \tanh(z) & \text{if } z \geq 0 \\ z & \text{otherwise} \end{cases}$$

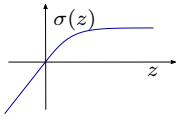

defining the new barrier functional

$$\beta_\delta(z) := \tilde{\beta}_\delta(\sigma(z))$$

that behaves as the standard barrier function $\tilde{\beta}_\delta$ for small and negative z, but goes to zero for $z \to \infty$ (Saccon et al., 2012).

4.2 The Optimization Problem

Our goal is to minimize the energy spent by each vehicle when moving from a given initial to a given final configuration. Using (9), the total power consumption of the i-th vehicle is

$$l_{\text{pow}}(\mathbf{x}^{[i]}(t), \mathbf{u}^{[i]}(t)) = \left(R_a I_{\text{ps}}^{[i]}(t) + K_e n_{\text{ps}}^{[i]}(t)\right) I_{\text{ps}}^{[i]}(t) + \left(R_a I_{\text{sb}}^{[i]}(t) + K_e n_{\text{sb}}^{[i]}(t)\right) I_{\text{sb}}^{[i]}(t) + P_p \quad (13)$$

where $\mathbf{x}^{[i]}(t)$ denotes the i-th vehicle's state vector. An additional cost term expressing L_2 trajectory optimization can be formulated as

$$l_{\text{des}}(\mathbf{x}^{[i]}(t), \mathbf{u}^{[i]}(t), t) = \frac{1}{2}\left|\left|\mathbf{x}^{[i]}(t) - \mathbf{x}_{\text{des}}^{[i]}(t)\right|\right|_{Q_{\text{to}}}^2 + \frac{1}{2}\left|\left|\mathbf{u}^{[i]}(t) - \mathbf{u}_{\text{des}}^{[i]}(t)\right|\right|_{R_{\text{to}}}^2 \quad (14)$$

where Q_{to} and R_{to} are positive definite weight matrices that have to be chosen appropriately.

The inter-vehicle collision avoidance constraint (explained in more detail in Saccon et al. (2012)) between vehicles i and j is

$$c_{\text{col}}(\mathbf{x}^{[i]}(t), \mathbf{x}^{[j]}(t)) = \frac{\left(x^{[i]}(t) - x^{[j]}(t)\right)^2}{(2r_{\text{c}})^2} + \frac{\left(y^{[i]}(t) - y^{[j]}(t)\right)^2}{(2r_{\text{c}})^2} - 1 \quad (15)$$

where r_{c} is the minimum safety distance that must be kept between two vehicles. Due to space limitations, the obstacle avoidance constraint $c_{\text{obs}}(\mathbf{x}^{[i]}(t), \mathbf{o}^{[k]})$ between vehicle i and obstacle k is not given here, but it can be formulated in a similar manner. (Here, $k \in \{1, \ldots, N_{\text{o}}\}$, where N_{o} is the total number of obstacles in the environment.)

Using the power function (13), the desired trajectory function (14), the inter-vehicle collision avoidance function (15), and the obstacle avoidance function, the vehicle trajectories are obtained by solving the optimization problem

$$\min \int_0^T \sum_{i=1}^{N_{\text{v}}} \Big(l_{\text{pow}}\big(\mathbf{x}^{[i]}(\tau), \mathbf{u}^{[i]}(\tau)\big) + l_{\text{des}}\big(\mathbf{x}^{[i]}(\tau), \mathbf{u}^{[i]}(\tau), \tau\big) \Big) d\tau + m(x(T))$$

$$\text{s.t. } \dot{\mathbf{x}}^{[i]} = f(\mathbf{x}^{[i]}, \mathbf{u}^{[i]}, t), \qquad \mathbf{x}^{[i]}(0) = \mathbf{x}_0^{[i]}, \mathbf{x}^{[i]}(T) = \mathbf{x}_{\text{f}}^{[i]}$$
$$c_{\text{col}}\big(\mathbf{x}^{[i]}(t), \mathbf{x}^{[j]}(t)\big) \geq 0, \; i \neq j$$
$$c_{\text{obs}}\big(\mathbf{x}^{[i]}(t), \mathbf{o}^{[k]}\big) \geq 0$$

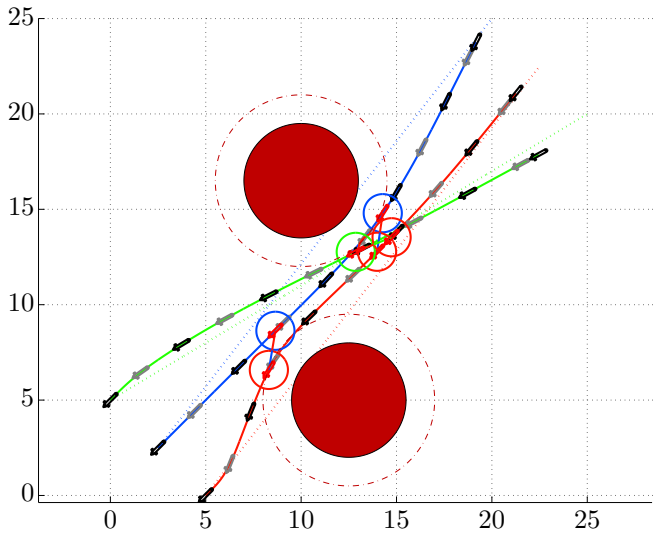

(a) The lines around the obstacles illustrate the safety distance of 1.5m between vessel and obstacle. The red vessel pictograms illustrate the point of closest proximity; the rings around the vessels indicate the inter-vessel safety distance of 2.0m. The desired trajectories are shown as dotted lines. Note that the vessels are drawn in their real sizes; the units on abscissa and ordinate axes are meters.

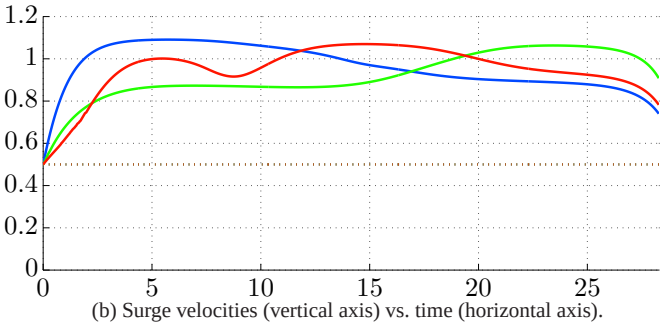

(b) Surge velocities (vertical axis) vs. time (horizontal axis).

Fig. 5. Three vessels and two obstacles. The scenario was deliberately chosen so that it initially would be infeasible (desired trajectories crossing obstacles and causing collisions) to show the planner's capability.

with $i, j \in \{1, \ldots, N_{\text{v}}\}$ and $k \in \{1, \ldots N_{\text{o}}\}$, and $\mathbf{x}_0^{[i]}$ and $\mathbf{x}_{\text{f}}^{[i]}$ are the initial and final condition on the i-th vehicle.

5. SIMULATION RESULTS

Due to space limitations, we restrict ourselves to one scenario that shows the capabilities of our motion planning approach in a scenario with three vehicles and two obstacles: the vehicles start at three arbitrary points and are required to arrive at three target points at exactly the same time T, following desired trajectories while avoiding collisions (see Fig. 5). The example shows that the projection operator approach is a very robust optimization method for our area of applictation: desired trajectories can be defined such that they intersect obstacles and would result in the vessels crashing into each other; the result in the end, however, is such that (a) the trajectories are "close" to the desired ones, while (b) being optimal with respect to energy expenditure, and (c) avoiding collisions with obstacles and between the vessels.

It is worth stressing that, in order to increase run-time efficiency and simplify the analytical expressions for first and second derivatives of a properly defined operator (as required by Newton's method), the four-quadrant thrust and torque coefficients (originally formulated as 20th order Fourier series) were approximated with 30-piece periodic cubic spline curves. Once

computed to machine precision, the spline coefficients can be stored in a C header file and need not to be recomputed at later runs of the algorithm. Of course, the algorithm can also be used for trajectory generation purposes by setting the weight matrices of the L_2 minimization part equal to zero.

6. CONCLUSIONS AND OUTLOOK

We presented a novel approach for multiple AMV trajectory optimization that is innovative in the following two main aspects:

- It is a solution finding process for a much extended problem formulation (including collision constraints, a novel thruster model, battery saving incremental cost, and explicit incorporation of the vessel model, while achieving simultaneous times of arrival).
- It is based on a projection operator method that allows applying a second order descent method, and, due to the nature of the approach, prior knowledge about the scenario is not required from the user in order to shape an initial guess.

In relation to previous work (Häusler et al., 2010) the new approach has the immediate advantages that (a) the algorithm can in general be expected to converge much faster than the previously adopted zero-order optimization, and that (b) we can quickly obtain a trajectory that is feasible both in terms of the vessel dynamics and in terms of the optimization constraints.

There are several issues that we plan to address in the immediate future: the influence of ocean currents on the paths has to be evaluated, and there are more constraints that may be incorporated, like e.g. communication constraints. In obstacle-rich environments, it would be preferable to only evaluate those obstacle avoidance constraints which are active to speed up the computation, which would require some (perhaps probabilistic) means of determining the "active obstacles", e.g Gottschalk et al. (1996). Aggressive maneuvering might make it necessary to incorporate constraints on the dynamic states or the inputs. Self-localization during an ongoing mission at sea (Teixeira and Pascoal, 2005) will be eased up by including terrain information already at the planning level, and mission performance metrics might be included as further terms in the cost function. Finally, it is highly desirable to soften up the problem associated with reaching the final boundary conditions by employing a root finding method Hauser (2003).

ACKNOWLEDGEMENTS

The authors would like to thank *Dr. Gert Kuiper*, formerly with Marin (Netherlands), for valuable insights into the nature of the four-quadrant thrust and torque coefficients, as well as *John Scanlon* from Seabotix for providing some crucial data on the brushless DC motors used in the Seabotix thrusters. Many thanks also go to *Luís Sebastião* for his elaborate and constructive remarks on the ongoing research.

REFERENCES

Aguiar, A., Almeida, J., Bayat, M., Cardeira, B., Cunha, R., Häusler, A., Maurya, P., Oliveira, A., Pascoal, A., Pereira, A., Rufino, M., Sebastião, L., Silvestre, C., and Vanni, F. (2009). A Cooperative Autonomous Marine Vehicle Motion Control in the Scope of the EU GREX Project: Theory and Practice. In *Proceedings of the IEEE Oceans '09*. Bremen, Germany.

Bachmayer, R., Whitcomb, L.L., and Grosenbaugh, M.A. (2000). An Accurate Four-Quadrant Nonlinear Dynamical Model for Marine Thrusters: Theory and Experimental Validation. *IEEE Journal of Oceanic Engineering*, 25(1), 146–159.

Chyba, M., Haberkorn, T., Smith, R.N., and Choi, S.K. (2008). Autonomous Underwater Vehicles: Development and Implementation of Time and Energy Efficient Trajectories. *Ship Technology Research*, 55(1), 36–48.

Fossen, T.I. (2002). *Marine Control Systems. Guidance, Navigation, and Control of Ships, Rigs, and Underwater Vehicles*. Marine Cybernetics, Trondheim, Norway.

Franklin, G.F., Powell, J.D., and Emami-Naeimi, A. (2002). *Feedback Control of Dynamic Systems*. Prentice Hall, 4th edition.

Gottschalk, S., Lin, M.C., D., and Manocha (1996). OBBTree: A Hierarchical Structure for Rapid Interference Detection. In *Proceedings of the 23rd Annual Conference on Computer Graphics and Interactive Techniques*, SIGGRAPH '96, 171–180. ACM, New York, NY, USA.

Hauser, J. (2002). A Projection Operator Approach to the Optimization of Trajectory Functionals. In *IFAC World Congress*. Barcelona, Spain.

Hauser, J. (2003). On the Computation of Optimal State Transfers with Application to the Control of Quantum Spin Systems. In *Proceedings of the 2003 American Control Conference*, volume 3, 2169–2174.

Hauser, J. and Saccon, A. (2006). A Barrier Function Method for the Optimization of Trajectory Functionals with Constraints. In *45th IEEE Conference on Decision and Control*, 864–869. San Diego, USA.

Häusler, A.J., Ghabcheloo, R., Pascoal, A.M., and Aguiar, A.P. (2010). Multiple Marine Vehicle Deconflicted Path Planning with Currents and Communication Constraints. In *7th IFAC Symposium on Intelligent Autonomous Vehicles*. Lecce, Italy.

Healey, A.J., Rock, S.M., Cody, S., Miles, D., and Brown, J.P. (1994). Toward an Improved Understanding of Thruster Dynamics for Underwater Vehicles. In *Proceedings of the 1994 Symposium on Autonomous Underwater Vehicle Technology*, 340–352.

Inanc, T., Shadden, S.C., and Marsden, J.E. (2005). Optimal Trajectory Generation in Ocean Flows. In *Proceedings of the American Control Conference (ACC 2005)*.

Indiveri, G., Antonelli, G., Caiti, A., Casalino, G., Birk, A., Pascoal, A., and Caffaz, A. (2010). The Co^3-AUVs Project: Overview and Current Progresses. In *7th IFAC Symposium on Intelligent Autonomous Vehicles*. Lecce, Italy.

Kruger, D., Stolkin, R., Blum, A., and Briganti, J. (2007). Optimal AUV Path Planning for Extended Missions in Complex, Fast-Flowing Estuarine Environments. In *2007 IEEE International Conference on Robotics and Automation*, 4265–4270.

Kumar, R.P., Dasgupta, A., and Kumar, C. (2005). Real-time Optimal Motion Planning for Autonomous Underwater Vehicles. *Ocean Engineering*, 32(11–12), 1431–1447.

Leonard, N.E., Paley, D.A., Davis, R.E., Fratantoni, D.M., Lekien, F., and Zhang, F. (2010). Coordinated Control of an Underwater Glider Fleet in an Adaptive Ocean Sampling Field Experiment in Monterey Bay. *Journal of Field Robotics*, 27(6), 718–740.

Ögren, P., Fiorelli, E., and Leonard, N.E. (2004). Cooperative Control of Mobile Sensor Networks: Adaptive Gradient Climbing in a Distributed Environment. *IEEE Transactions on Automatic Control*, 49(8), 1292–1302.

Oosterveld, M.W.C. (1970). *Wake Adapted Ducted Propellers*. Ph.D. thesis, Delft University of Technology, Wageningen, The Netherlands.

Paley, D.A., Zhang, F., and Leonard, N.E. (2008). Cooperative Control for Ocean Sampling: The Glider Coordinated Control System. *IEEE Transactions on Control Systems Technology*, 16(4), 735–744.

Saccon, A., Aguiar, A.P., Häusler, A.J., Hauser, J., and Pascoal, A.M. (2012). Constrained Motion Planning for Multiple Vehicles on $\mathbf{SE}(3)$. In *51st IEEE Conference on Decision and Control*. Maui, Hawai'i. Accepted.

Spangelo, I. and Egeland, O. (1994). Trajectory Planning and Collision Avoidance for Underwater Vehicles Using Optimal Control. *IEEE Journal of Oceanic Engineering*, 19(4), 502–511.

Teixeira, F. and Pascoal, A. (2005). AUV Terrain Aided Navigation using Particle Filters. In *Proc. of IWUR2005 - International Workshop on Underwater Robotics*. Genova, Italy.

van Lammeren, W.P.A., van Manen, J.D., and Oosterveld, M.W.C. (1969). The Wageningen B-Screw Series. *Transactions of SNAME*, 77, 269–317.